Atmospheric circulation influences on seasonal precipitation patterns in Alaska during the latter 20th century

Michelle L. L'Heureux

Department of Environmental Sciences, University of Virginia, Charlottesville, Virginia, USA

Now at Department of Atmospheric Science, Colorado State University, Fort Collins, Colorado, USA

Michael E. Mann and Benjamin I. Cook

Department of Environmental Sciences, University of Virginia, Charlottesville, Virginia, USA

Byron E. Gleason and Russell S. Vose

National Climatic Data Center, NOAA/National Environmental Satellite Data and Information Service, Asheville, North Carolina, USA

[1] A set of long, nearly complete daily precipitation series for Alaska spanning the latter half of the 20th century has been analyzed for seasonal relationships between variations in mean, heavy, and extreme precipitation and large-scale atmospheric circulation variations at interannual, decadal, and secular timescales. Relationships with four candidate predictors (the Pacific North American (PNA), Arctic Oscillation (AO), Pacific Decadal Oscillation (PDO), and Nino3 indices) are used for insights into possible large-scale climate forcing. Winter precipitation (mean and extreme) variability and trends along the south coast and interior of Alaska appear to be closely related to variations in the PNA pattern over this timeframe, while El Nino/Southern Oscillation (ENSO) influences, through the Nino3 index, appear to be significant along the south coast alone. Along the south coast the PNA and ENSO exert opposing influences on extreme (and mean) precipitation. Within interior Alaska the positive PNA pattern tends to suppress precipitation owing to orographic factors. Summer variations appear more closely related to the influence of the AO and PDO. The north slope region of Alaska appears to be too far removed from the influences of any of the examined predictors for any clear relationship to be evident.   *INDEX TERMS:* 3309 Meteorology and Atmospheric Dynamics: Climatology (1620); 3319 Meteorology and Atmospheric Dynamics: General circulation; 3354 Meteorology and Atmospheric Dynamics: Precipitation (1854); *KEYWORDS:* Alaska, precipitation, circulation, climate variability, climate change, PNA

1. Introduction and Background

[2] Significant changes in Alaskan climate have taken place during the 20th century. In some regions of Alaska, these changes are documented through dramatic mountain glacier recession, extended growing season length, and thawing of permafrost. The observed climate trends are, however, highly variable regionally, and with respect to the particular time interval and season examined. Since the mid 20th century, there has been significant warming in the north slope region of Alaska, particularly in summer, and significant warming along the south coast of Alaska. In contrast, much of the interior of Alaska has exhibited summer warming, but winter trends are more variable, indicating cooling in some areas over several decades [*Folland et al.*, 2001], but warming in most regions over the past 25 years. The overall warming tendency is consistent with larger-scale 20th century warming trends that may have an anthropogenic component [*Watson*, 2001], while the more variable winter temperature changes may have a strong atmospheric circulation component [e.g., *Trenberth*, 1990; *Hurrell and van Loon*, 1997]. Notable variations in hydroclimatic variables have also been observed in Alaska over this time period. Consistent with trends throughout the western Arctic region, the frequency and intensity of daily precipitation on the north slope of Alaska has decreased between 1950–1988, especially during the winter months [*Curtis et al.*, 1998]. Elsewhere in Alaska, mean annual precipitation has either increased slightly or has changed little [*Groisman and Easterling*,
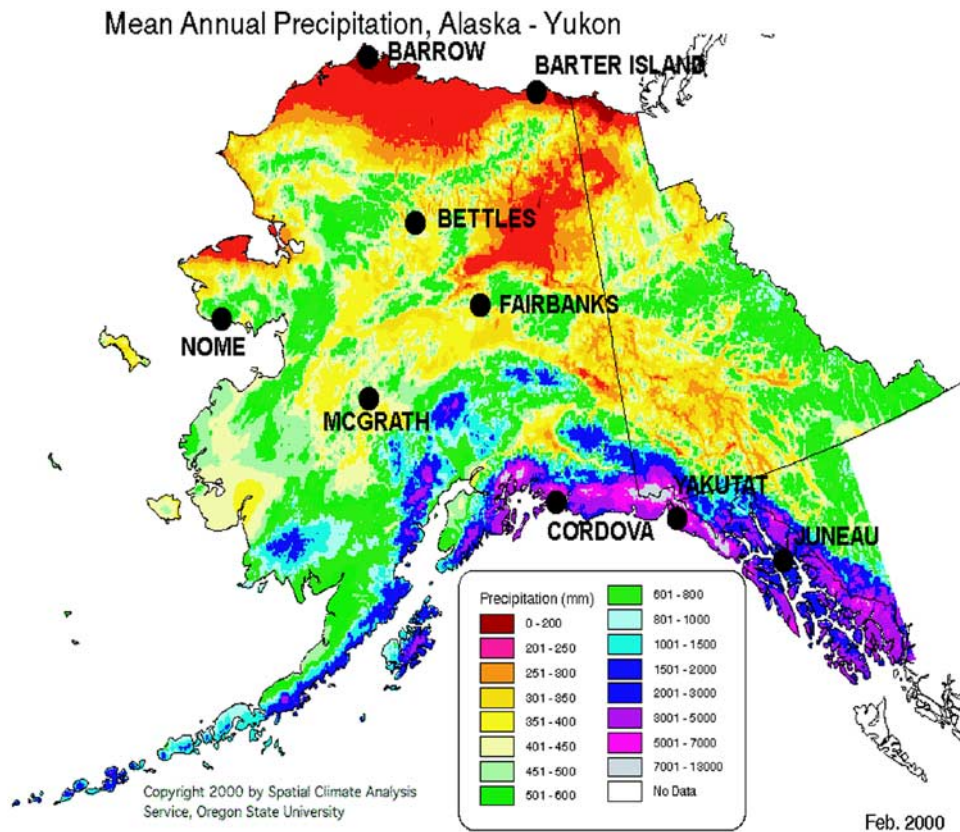
Figure 1. Climatological pattern of annual mean precipitation over Alaska. The locations of the nine stations are noted. The map is duplicated with permission from the Spatial Climate Analysis Service and uses a state-of-the-art digital elevation model (PRISM) that interpolates precipitation between station observations encompassing Alaska [*Daly et al.*, 1994]. Image courtesy of the Spatial Climate Analysis Service, Oregon State University (http://www.ocs.oregonstate.edu/prism).

1994], with the main increases observed during the most recent decades, and moderate decreases found during the mid 20th century [*Folland et al.*, 2001]. These observations suggest significant variability on decadal timescales in the factors underlying observed precipitation variations.

[3] Mean annual precipitation varies dramatically across Alaska (Figure 1), from less than 200 mm at the northern end to just over 8000 mm in some southern regions [*Paulson et al.*, 1991]. Much of this variation arises from orographic influences. Most of southern Alaska's annual precipitation occurs on the windward side of the coastal range, which runs zonally along the southern coast. From west to east, the Aleutian Range, the Alaska Range, and the Coast Range form a natural barrier to the moisture associated with inflow of maritime air from the Pacific Ocean. These mountain ranges are sizable (Mt. McKinley of the Alaska Range, for example, has an elevation of 20,320 feet) and can exert a considerable rain-shadow effect. Just north of the southern ranges are the low-lands of Alaska, which are not devoid of moisture because ocean moisture can reach inward from the west [*Bowling*, 1980]. Yet another mountain range, the Brooks Range, extends horizontally across the northern region of the state. The peaks of the Brooks Range average around 7000 feet with its largest peaks in the east, tapering off to the west. The north slope is Arctic tundra that receives very little precipitation due to the Brooks Range in the south, and the Beaufort Sea to the

north, which during the winter, can effectively become an extension of the north slope due to a covering of sea ice [*Bowling*, 1980]. Thus Alaska can be easily subdivided into at least three climate zones subdivided by the natural terrain and typical annual precipitation.

[4] Here we document the likely importance of regional, seasonal atmospheric circulation changes on interannual and decadal timescales in governing observed variations in Alaskan precipitation patterns during the latter half of the 20th century. It is clear that any changes in prevailing wind patterns, air mass regimes, or moisture sources must interact with the complex orography in determining the influence of atmospheric circulation variations on large-scale hydroclimatology in Alaska. Thus, in seeking to understand observed precipitation trends at a more fundamental level, we will examine the extent to which seasonal precipitation relate to the larger-scale patterns of climate influence within an explicit geographic context. This contrasts with analyses focusing on gridded regional precipitation trends [*Hulme et al.*, 1998; *Doherty et al.*, 1999; *Folland et al.*, 2001]. Based on the three distinct precipitation zones discussed above, we examine precipitation trends for stations located (a) on the north slope, (b) between the northern and southern mountain ranges, and (c) along the southern coast. Heavy precipitation may be more closely associated with any underlying climate variability than mean precipitation itself [*Katz and Brown*,
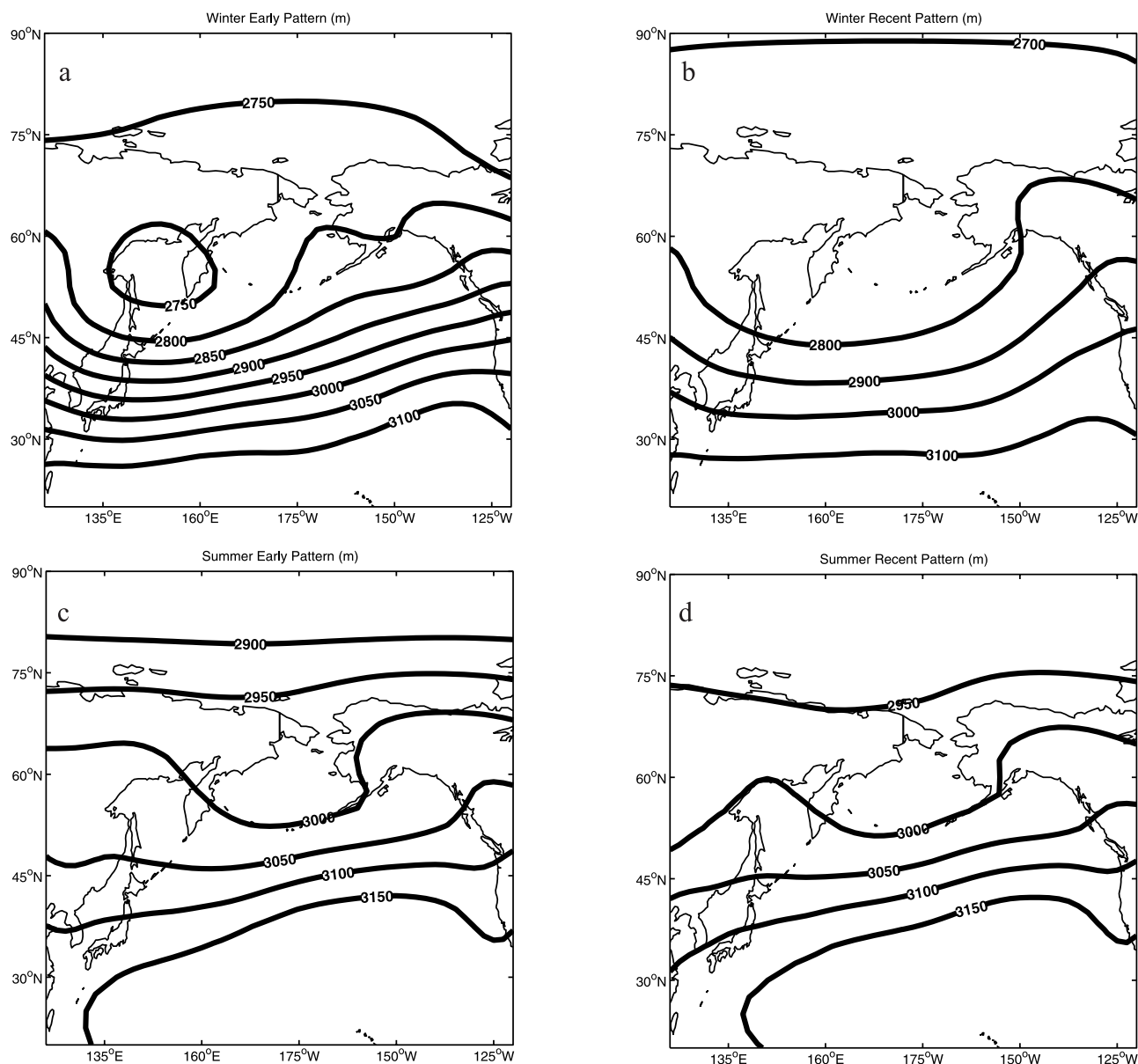
Figure 2. 700 hPa winter climatology for (a) the early pattern (minus half the trend) and (b) recent pattern (plus half the trend). Same for the 700 hPa summer climatology (c) minus and (d) plus half the trend.

1992] and previous studies have found, for example, that the roughly 10% observed increase for the contiguous United States during the 20th century [*Karl and Knight*, 1998] appears to be largely associated with an increase in the amount of precipitation associated with "very heavy" (exceeding the 90th percentile) precipitation days [*Karl and Knight*, 1998]. We thus choose to examine variations in trends in heavy, as well as mean, precipitation. The prevailing large-scale atmospheric circulation patterns influencing Alaska vary dramatically with season (Figure 2). Therefore we examine the relationship between observed precipitation and atmospheric circulation variations separately for both winter and summer seasons. The transitional (spring and autumn) seasons are not investigated here.

[5] We seek to establish the separate apparent influences of various modes of North Pacific climate variability on Alaskan precipitation. Our analysis approach involves a multivariate regression employing a pool of candidate climate indices as predictors: the Pacific North American pattern (PNA) [see *Wallace and Gutzler*, 1981], the Pacific Decadal Oscillation (PDO) [see *Mantua et al.*, 1997], the Arctic Oscillation (AO) [see *Thompson and Wallace*, 1998; *Thompson and Wallace*, 2000], and the NINO3 index [see, e.g., *Trenberth*, 1997]. These four indices represent both tropical and extratropical climate processes potentially influencing atmospheric circulation and precipitation patterns in the North Pacific. As these indices are not statistically independent, we use a traditional multivariate linear regression to attempt to isolate their partial influences on Alaskan
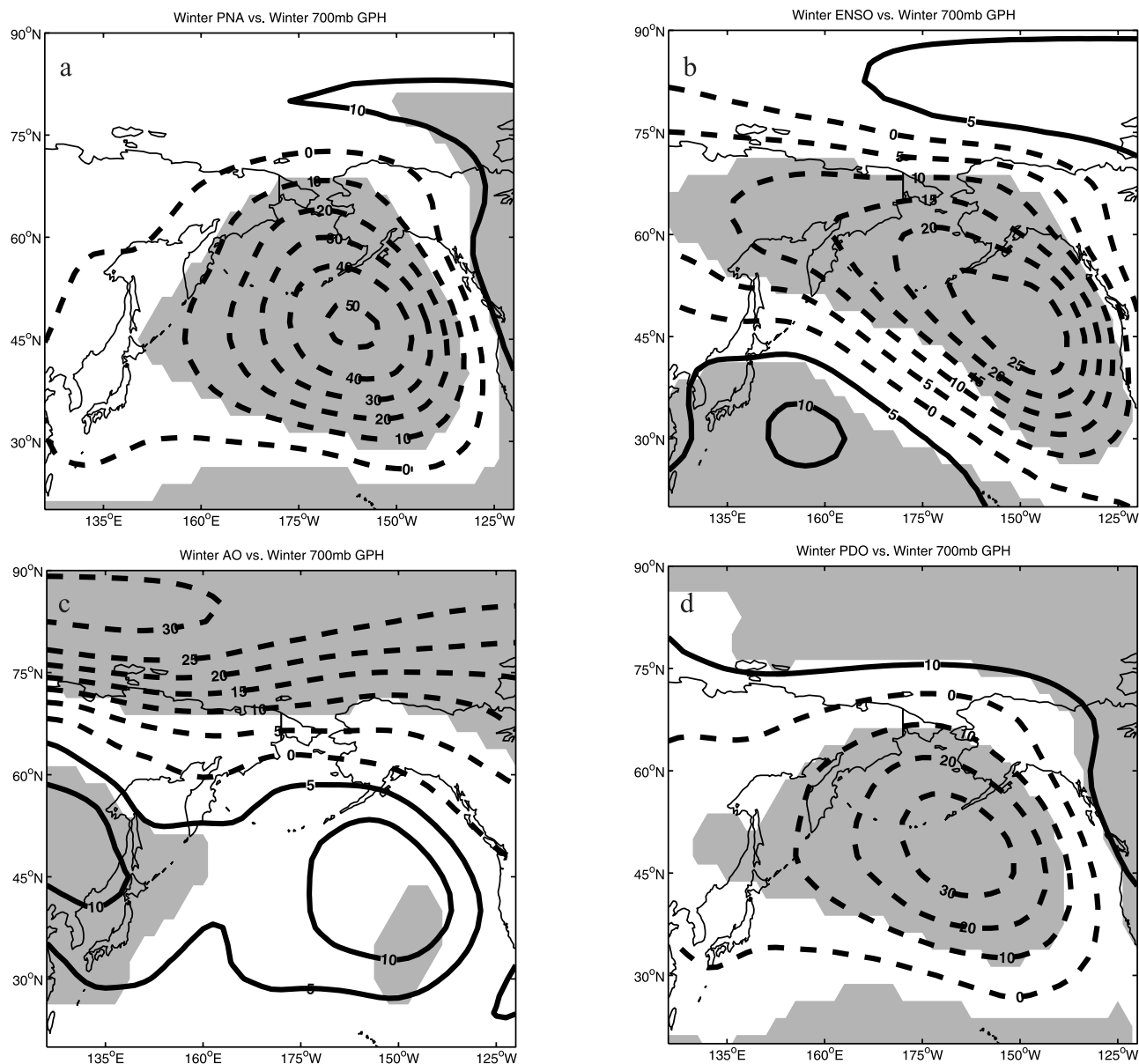
Figure 3. Winter 700 hPa geopotential heights regressed onto the winter (a) PNA (b) NINO3 (c) AO (d) PDO (negative and zero contours are dashed; shading represents 95% confidence using the two-tailed t-distribution).

precipitation. This set of 4 indices reasonably spans the degrees of freedom of climate variability in the North Pacific on interannual and longer timescales. A Principal Component Analysis (PCA) of these indices suggests that they span at least 3 degrees of freedom of the interannual variability of both winter and summer seasons (the first 3 eigenvalues are significantly different from zero). By comparison, a PCA of an expanded set of eight indicators (including additionally the SOI, TNH, NP, WP teleconnection indices) [see, e.g., *Barnston and Livezey*, 1987] reveals that the first three (four) eigenvalues resolve 75% (87%) of the interannual variance during the cold season and 67% (79%) during the warm season, motivating the use of the more modest set of 4 indices. Atmospheric circulation variability in the extratropical North Pacific certainly exhibits a greater number of degrees of freedom on intraseasonal

timescales, and the four indices chosen (PNA, PDO, AO, and NINO3) by no means comprise a unique set of descriptors of extratropical North Pacific climate. The 4 indices do nonetheless provide a convenient, low-dimensional set of predictors of interannual and decadal climate variability in the extratropical North Pacific.

[6] The PNA, PDO, AO, and NINO3 thus comprise a convenient set of climate indices plausibly linked to changes in Alaskan precipitation on interannual and longer timescales. The PNA index represents a mode of variability in the upper level height field associated with internal midlatitude atmospheric dynamics and first described by *Wallace and Gutzler* [1981], who noted its four centers of action. Anomalies of similar sign are located over the southeastern United States and just south of the Aleutian Islands, while anomalies of opposite sign are located in
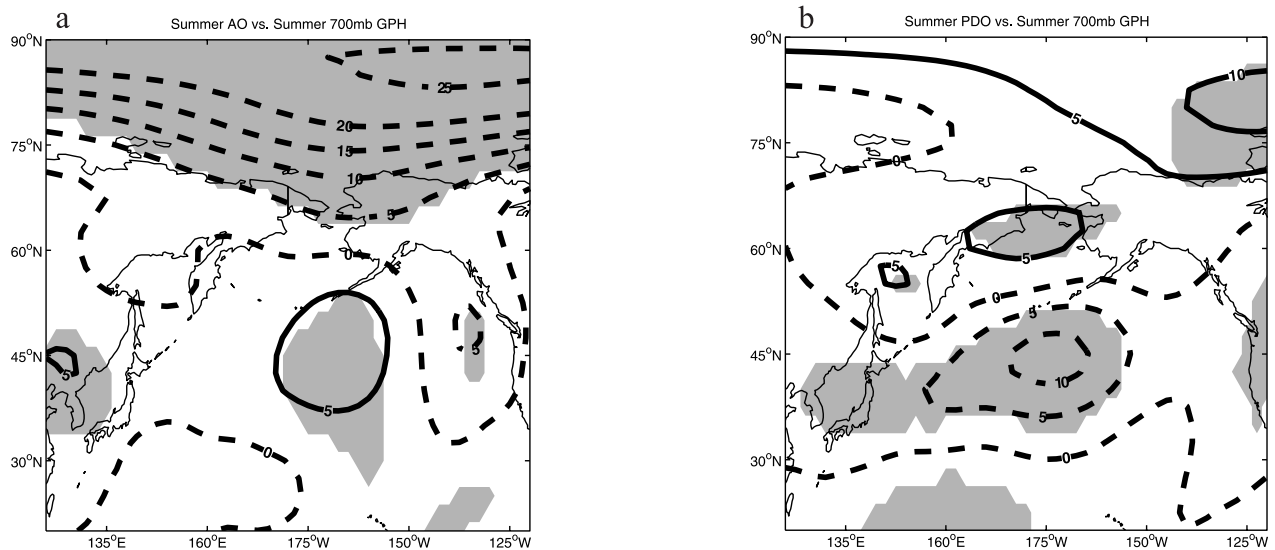
Figure 4. Summer 700 hPa geopotential heights regressed onto the summer (a) AO (b) PDO (negative and zero contours are dashed; shading represents 95% confidence using the two-tailed t-distribution).

the Hawaiian region and over central Canada. *Cayan and Peterson* [1989] identify an influence of the Pacific North American (PNA) pattern influence on streamflow patterns (which are tied, in large part, to seasonally integrated precipitation) in southern coastal Alaska. ENSO, through its established influence on extratropical North Pacific atmospheric circulation, is an obvious candidate predictor. The winter PNA and NINO3 are correlated ($r = 0.59$), consistent with some degree of established relationship between ENSO and the winter PNA [*Renshaw et al.*, 1998], which appears to result from the conditioning of the PNA by tropical Pacific SSTs [*Livezey and Mo*, 1987]. An incontrovertible physical interpretation of the PDO [see *Mantua et al.*, 1997], is not yet possible. While spatially similar to ENSO, the variability associated with the PDO may be governed by distinct extratropical ocean-atmosphere processes [*Trenberth and Hurrell*, 1994], low-frequency ENSO-like variability, or simple stochastic variability of the climate [e.g., *Miller and Schneider*, 2000; *Mantua and Hare*, 2002]. The available instrumental record is too short to establish if there is indeed even a preferred timescale of variation to the PDO. The positive (warm) phase of the PDO is characterized by more pronounced cooling in the central extratropical North Pacific, and a weaker, but meridionally broader pattern of eastern tropical Pacific warming in the tropical Pacific than ENSO. The warm phase of the PDO, as the warm phase of ENSO and the PNA, is associated with a winter pattern of an enhanced Aleutian low [*Trenberth*, 1990]. The AO [see *Thompson and Wallace*, 1998; *Thompson and Wallace*, 2000] is the surface expression of the annular mode of atmospheric variability associated with variations in the strength of the upper-level circumpolar vortex in the Northern Hemisphere. The positive phase is associated with strengthened tropospheric subpolar westerlies and a more zonal flow [*Thompson and Wallace*, 1998]. Strengthened subpolar westerlies could ostensibly increase precipitation in coastal and windward interior regions of Alaska through enhanced advection of mild, maritime Pacific air [see *Hurrell and van Loon*, 1997].

[7]   In section 2, we describe the data used in this study. In section 3, we describe our analysis methods. In section 4, we discuss the results of the analysis, and we present our conclusions in section 5.

2.   Data

2.1.   Precipitation Data

[8]   Precipitation data were obtained from the National Climatic Data Center, and includes daily precipitation records since the beginning of the measuring period for nine Alaskan stations: Barrow, Barter Island, Bettles, Fairbanks, Nome, McGrath, Cordova, Yakutat, and Juneau (from north to south). These stations are selected based on geographic variety, measurement longevity, and data completeness. Figure 1 locates the stations on a spatial map of mean annual precipitation over Alaska. The precipitation data is analyzed separately during the winter (DJF) and summer (JJA) seasons. It is worth noting that gauges used in precipitation measurements in the north slope region may underestimate snowfall accumulation [*Curtis et al.*, 1998]. This effect likely imposes a bias in the estimates of climatological mean precipitation in these regions, but less obviously in the relative pattern of variation in precipitation over time, which is of interest in the current study. However, the underestimates of snowfall accumulation could lead to a reduced precipitation signal in the winter season, hampering efforts to relate observed precipitation variability to under-

Table 1.   Trends of the Four Indices (PNA, AO, NINO, and PDO) Over the 1950–1998 Timeframe in Standardized Units

Trend	1950–1998	
	Winter	Summer
PNA	0.8	−0.1
AO	1.2	0.7
PDO	1.7	2.0
NINO	0.8	

Table 2a. Multivariate Correlations of the Undetrended Standardized Predictors (PNA, AO, PDO, NINO3) Against Transformed, Undetrended, Heavy (90–95%), Extreme (95–100%), and Mean Alaskan Precipitation During 1950–1998 (Juneau, Fairbanks, Barrow, and Cordova), 1950–1988 (Barter Island), and 1952–1998 (Bettles) During the Winter Season[a]

Partial r	1950–1998							1950–1988	1952–1998
	Nome	McGrath	Yakutat	Barrow	Cordova	Fairbanks	Juneau	Barter	Bettles
90–95%									
PNA	0.3283	**−0.5311**	0.1599	−0.0443	**0.4897**	**−0.5547**	0.0729	0.3159	−0.2147
AO	0.2007	*0.2337*	0.1268	0.0725	0.1759	*0.2281*	**0.2845**	−0.0949	**0.4086**
PDO	0.1633	0.2467	0.2896	0.1275	0.1015	0.1239	*0.3395*	−0.3283	**0.6215**
NINO	**−0.3522**	−0.1397	−0.1531	−0.1578	−0.1831	0.0139	−0.2208	0.0091	0.0629
95–100%									
PNA	−0.1189	**−0.4854**	0.3109	−0.1213	**0.6903**	**−0.5608**	0.0828	0.0522	−0.1232
AO	**0.302**	**0.2984**	0.2898	−0.1121	**0.3351**	−0.1285	**0.3435**	−0.0397	0.1127
PDO	0.0789	0.0836	*0.322*	−0.3396	0.0869	−0.0266	*0.356*	−0.2113	0.2223
NINO	0.0118	−0.0516	*−0.3441*	−0.046	**−0.4283**	0.1201	−0.2657	−0.24	−0.1405
Mean									
PNA	−0.1404	**−0.4618**	0.4413	−0.1113	**0.6985**	**−0.6498**	0.1049	0.0793	−0.0611
AO	*0.2857*	**0.3331**	*0.2433*	−0.077	**0.2796**	−0.031	**0.2993**	−0.0331	*0.2535*
PDO	0.1989	0.1379	0.2873	−0.2171	0.1316	0.035	*0.3615*	−0.2633	−0.2091
NINO	−0.0293	−0.1208	*−0.2771*	−0.1077	**−0.32**	0.1076	*−0.2933*	−0.2046	−0.0971

[a]Boldface indicates significance greater than 95%, and italics indicate significance greater than 90%. R-squared values greater than 0.20 are also in boldface. Additional information: R-squared is the coefficient of determination (fraction of variance resolved) by the regression with all 4 indices. The *f* ratio measures the ratio of regression and residual variance per statistical degree of freedom, and "p" represents the probability with which the null hypothesis of no relationship with the candidate predictors can be rejected.

lying large-scale winter climate variations in the north slope region.

[9] The precipitation analysis includes 49 winters (DJF 1949–1998) and 49 summers (JJA 1950–1998) for all stations except for Barter Island, which was taken offline in 1988, and Bettles, where observations began in 1952. Subsequently, Barter Island precipitation analysis is restricted to 39 summer seasons and 39 winter seasons between 1949–88, and Bettles is restricted to 47 summer seasons and 47 winter seasons between 1952–1998. Some short gaps in the records (Juneau (JJA 1968), Cordova (Jan. 1991), McGrath (JF 1964), Bettles (JF 1998, June 1974, July 1959, Aug. 1996)) were infilled with the appropriate climatological monthly mean precipitation estimates. In addition to looking at the "mean" or cumulative seasonal precipitation, "heavy" and "extreme" precipitation categories are constructed using the method defined by *Karl and Knight* [1998]. Within a season, each day is ranked accord-

ing to precipitation amount, and those days that are ranked within the top 5% are summed. We adopt the convention of classifying the 95–100% bin as the "extreme" precipitation category for consistency with previous studies [*Karl and Knight*, 1998]. Similarly, we classify the 90–95% percentile bin as the "heavy" precipitation category.

[10] Because many of the seasonal precipitation estimates used either represent (e.g., in the north slope region) low seasonal accumulation, or (in the case of "heavy" and "extreme" precipitation estimates for all stations) averages over a small number of precipitation events, the data typically do not satisfy the requirements of the central limit theorem. A suitable transformation yielding an approximately normal distribution must thus be applied to the associated time series prior to applying of standard linear regression methods and associated significance estimation procedures. It was found that a square root transformation yielded approximate normally distributed time series in

Table 2b. Multivariate Correlations of the Undetrended Standardized Predictors (PNA, AO, PDO, NINO3) Against Transformed, Undetrended, Heavy (90–95%), Extreme (95–100%), and Mean Alaskan Precipitation During 1950–1998 (Juneau, Fairbanks, Barrow, and Cordova), 1950–1988 (Barter Island), and 1952–1998 (Bettles) During the Winter Season[a]

Statistics	90–95%			95–100%			Cumulative Mean		
	R-Squared	*f* Ratio	*p*	R-Squared	*f* Ratio	*p*	R-Squared	*f* Ratio	*p*
Nome	0.1579	2.812	0.05	0.1022	1.7071	0.179	0.0986	1.6414	0.1932
McGrath	**0.3119**	6.8003	0.0007	**0.3409**	7.7596	0.0003	**0.3542**	8.2272	0.0002
Yakutat	0.1305	2.251	0.0953	**0.2672**	5.4688	0.0027	**0.3257**	7.2458	0.0005
Barrow	0.0296	0.4576	0.7133	**0.2083**	3.9477	0.0139	0.1384	2.4088	0.0794
Cordova	**0.2306**	4.4957	0.0077	**0.4011**	10.0454	0	**0.443**	11.9295	0
Fairbanks	**0.302**	6.4889	0.001	**0.2613**	5.3048	0.0032	**0.3182**	7.0004	0.0006
Juneau	0.1675	3.0191	0.0395	**0.2124**	4.0459	0.0125	**0.2023**	3.8036	0.0163
Barter	0.0601	0.746	0.532	0.1201	1.592	0.2088	0.1163	1.5354	0.2225
Bettles	**0.3872**	9.0548	0.0001	0.0507	0.7661	0.5193	0.1824	3.1984	0.0327

[a]Boldface indicates significance greater than 95%, and italics indicate significance greater than 90%. R-squared values greater than 0.20 are also in boldface. Additional information: R-squared is the coefficient of determination (fraction of variance resolved) by the regression with all 4 indices. The *f* ratio measures the ratio of regression and residual variance per statistical degree of freedom, and "p" represents the probability with which the null hypothesis of no relationship with the candidate predictors can be rejected.

Table 3a. Same as Table 2a Except for the Summer Season

| Partial r | 1950–1998 | | | | | | | 1950–1988 | 1952–1998 |
	Nome	McGrath	Yakutat	Barrow	Cordova	Fairbanks	Juneau	Barter	Bettles
					90–95%				
PNA	−0.1376	0.0856	−0.1361	0.053	0.0518	0.0222	−0.0576	−0.0621	0.055
AO	0.0668	−0.0283	0.0316	−0.054	0.0469	0.0291	0.1445	−0.1332	**0.2929**
PDO	−0.0358	−0.0425	−0.2524	−0.0076	0.0179	−0.1971	0.0448	0.0291	**0.5918**
NINO	−0.0603	0.0658	0.1963	−0.1252	0.0861	−0.1188	0.2462	−0.0978	0.017
					95–100%				
PNA	−0.0379	0.0467	−0.1101	0.0595	−0.1127	0.1617	0.0155	0.1144	−0.1284
AO	**0.3239**	0.1808	0.0876	−0.0926	0.0105	0.204	0.0387	0.2355	0.2055
PDO	−0.0657	*−0.2558*	0.0931	−0.0827	0.0835	−0.2298	−0.1143	**−0.3807**	0.1431
NINO	−0.0066	*0.2496*	0.1142	−0.0607	0.0617	0.1622	0.1682	−0.0986	−0.0605
					Mean				
PNA	−0.0717	0.0513	−0.1827	0.0825	−0.1287	0.1584	0.0335	0.0831	**−0.2935**
AO	**0.3069**	0.158	0.1097	−0.0235	−0.0072	0.224	0.0444	0.2138	0.1861
PDO	−0.1049	−0.2087	−0.0309	−0.0358	0.0263	*−0.2912*	−0.1194	**−0.3906**	−0.0248
NINO	0.0036	0.2384	0.1682	−0.0742	0.159	0.1869	0.2161	−0.0441	0.1998

almost all cases after removal of any statistically significant trends in the transformed data. For the north slope winter precipitation series, the distributions of the transformed data show some slight evidence of departure from normality ($p = 0.10$), but not enough so as to introduce any serious problems in drawing appropriate inferences from a traditional ANOVA. As expected, transformed precipitation series for stations in regions receiving more frequent seasonal precipitation (Fairbanks, Nome, McGrath, Cordova, Yakutat, and Juneau) exhibit more closely a normal distribution.

2.2. Climate Indices

[11] The PNA, PDO, and AO climate indices were obtained for both the winter (DJF) and summer (JJA) seasons for comparison against the corresponding seasonal transformed precipitation series (for example, summer precipitation series are compared against the summer PNA, summer PDO, and summer AO). In contrast, only the conventional winter season (DJF) was used to define the NINO3 index (constructed as the average tropical Pacific sea surface temperature (SST) anomaly in the NINO3 region (5°N–5°S, 150°W–90°W) using the SST data of *Jones et al.* [1999]) for use in both seasonal analyses. The standardized PNA index was obtained from the criteria outlined in the work of *Wallace and Gutzler* [1981], which calculates the PNA based on 500mb grid points that are defined

"centers of action." The PDO index of *Mantua et al.* [1997] was employed, defined as the leading principal component of monthly SST anomalies in the North Pacific Ocean poleward of 20°N following removal of monthly global mean SST [*Mantua et al.*, 1997]. The latter step yields a measurement of variations in North Pacific SST relative to the overall pattern of global surface warming. The standardized seasonally resolved AO index of *Thompson and Wallace* [2000] was employed, defined as the leading seasonal pattern of extratropical Northern Hemisphere SLP variability.

2.3. 700 hPa Geopotential Height Data

[12] As in other past studies [e.g., *Barnston and Livezey*, 1987], we classify the low-frequency extratropical atmospheric circulation though an analysis of the 700 hPa geopotential height field. The 700 hPa heights represent a compromise between capturing summertime low-level moisture flow and wintertime synoptic variability, and avoiding topography. We make use of the 2.5-degree latitude by longitude gridded monthly mean 700 hPa geopotential height data from the NCEP/NCAR reanalysis project [*Kalnay*, 1996]. The full dataset spans the entire global domain back to 1948. The reanalysis data uses state of the art weather forecasting model to assimilate past available meteorological data into a dynamically consistent estimate of spatially complete meteorological fields. Poten-

Table 3b. Same as Table 2b Except for the Summer Season

| Statistics | 90–95% | | | 95–100% | | | Cumulative Mean | | |
	R-Squared	*f* Ratio	*p*	R-Squared	*f* Ratio	*p*	R-Squared	*f* Ratio	*p*
Nome	0.0306	0.4738	0.7021	0.1181	2.0081	0.1263	0.1208	2.0605	0.1189
McGrath	0.0128	0.1947	0.8994	0.1379	2.4004	0.0802	0.1081	1.8179	0.1575
Yakutat	0.0868	1.4262	0.2476	0.048	0.7565	0.5244	0.0728	1.1772	0.329
Barrow	0.0223	0.3419	0.7952	0.0247	0.3801	0.7678	0.016	0.2444	0.8649
Cordova	0.0134	0.2035	0.8934	0.0278	0.4294	0.7329	0.0451	0.7079	0.5523
Fairbanks	0.0718	1.1607	0.3352	0.1414	2.4701	0.074	0.1854	3.414	0.0252
Juneau	0.094	1.5558	0.2132	0.0323	0.501	0.6835	0.0497	0.7849	0.5087
Barter	0.0324	0.3912	0.7601	**0.2929**	4.8335	0.0064	**0.2568**	4.032	0.0145
Bettles	**0.3763**	8.6493	0.0001	0.0695	1.0705	0.3716	0.1576	2.6813	0.0587

Table 4a. Multivariate Correlations of Detrended Predictors Against Transformed Detrended Precipitation Categories During the Winter Season

Partial r	1950–1998							1950–1988	1952–1998
	Nome	McGrath	Yakutat	Barrow	Cordova	Fairbanks	Juneau	Barter	Bettles
90–95%									
PNA	*0.3693*	−0.4863	0.2058	−0.0302	**0.5003**	−0.5714	0.1011	0.1261	−0.1443
AO	0.1194	0.1568	0.0435	0.0437	0.1447	**0.2746**	0.2293	−0.0211	−0.1833
PDO	0.0327	0.1191	0.1419	0.0744	0.0533	0.1989	0.2336	0.1194	0.112
NINO	**−0.3687**	−0.1497	−0.1722	−0.1585	−0.1872	0.0252	−0.2349	0.0031	−0.1254
95–100%									
PNA	−0.0874	**−0.401**	**0.4571**	−0.2999	**0.7594**	**−0.5264**	0.1471	−0.0826	−0.1339
AO	0.232	0.1248	0.1167	0.1589	*0.2493*	−0.1612	0.2405	0.0122	0.1288
PDO	−0.0177	−0.1761	0.0232	0.0696	−0.0504	−0.0838	0.1692	0.0892	0.2338
NINO	0.0003	−0.0845	**−0.429**	0.001	**−0.4602**	0.1094	*−0.3044*	−0.2559	−0.1344
Mean									
PNA	−0.0957	**−0.3857**	**0.5435**	−0.2578	**0.7836**	**−0.5997**	0.1714	−0.0551	−0.0684
AO	0.1915	0.1738	0.1273	0.1668	0.191	−0.0888	0.1911	0.0194	*0.2528*
PDO	0.0468	−0.1043	0.0864	0.1598	−0.0178	−0.06	0.1691	0.0447	−0.1665
NINO	−0.0471	−0.1513	**−0.3245**	−0.0729	**−0.3551**	0.0929	*−0.3328*	−0.2203	−0.093

tial biases and errors in the dataset are discussed elsewhere [*Hurrell and Trenberth*, 1998; *Kistler et al.*, 2001]. While the reliability of the NCEP dataset for the determination of trends (particularly, in temperatures), has been called into question [*Hurrell and Trenberth*, 1998], our primary use of the NCEP data, the determination of composites of extreme daily events, is unlikely to be impacted by the biases involved. Where we do interpret trends in the NCEP (geopotential height) data, we verify that other independent data sources (e.g., SLP data from *Trenberth and Paolino* [1980] provide similar insights). We confine our analysis of the dataset to the North Pacific region bounded by 20°N and 90°N of latitude, 120°W and 120°E of longitude.

3. Methods

[13] We employ two distinct statistical approaches to establishing the nature of the relationship between large-scale atmospheric influences and Alaskan precipitation variations and trends. First, we perform a multivariate regression of the transformed precipitation series against various candidate climate indices (both for raw and detrended series). Second, we evaluate the large-scale spatial patterns of anomalous atmospheric circulation (as indicated by the 700 hPa geopotential height field) associated with the various indices (and with the late 20th century trend), and we interpret the anomalous atmospheric circulation associated with composites of extreme/heavy categorical precipitation days for insights.

3.1. Multivariate Regression Against Climate Indices

[14] As the four candidate predictors, the PNA, PDO, AO, and NINO3 series are not statistically independent (the PNA, PDO, and NINO3 predictors, in particular, exhibit significant mutual correlation), a multivariate linear regression approach must be employed to estimate the partial influences of each of the four candidate predictors. Such a multivariate regression eliminates the spurious possible inferences that might be drawn from simple individual correlations when, as in this case, substantial correlations between these individual predictors can lead to one index masquerading as a significant predictor of precipitation changes by virtue of its correlation with an index exhibiting a stronger (and thus, more likely, meaningful) correlation. We employed a multivariate regression of the transformed station precipitation data (mean, heavy, and extreme precipitation), using the standardized PNA, PDO, AO, and NINO3 indices as predictors of the standardized, transformed precipitation series. We stress the caveat that the 50-year interval considered might not span the full range of

Table 4b. Multivariate Correlations of Detrended Predictors Against Transformed Detrended Precipitation Categories During the Winter Season

Statistics	90–95%			95–100%			Cumulative Mean		
	R-Squared	*f* Ratio	*p*	R-Squared	*f* Ratio	*p*	R-Squared	*f* Ratio	*p*
Nome	0.1226	2.0966	0.114	0.0775	1.2603	0.2994	0.0519	0.8219	0.4887
McGrath	**0.3162**	6.9352	0.0006	**0.4066**	10.2761	0	**0.3995**	9.9799	0
Yakutat	0.0684	1.1007	0.3587	0.1708	3.089	0.0364	**0.2316**	4.5213	0.0074
Barrow	0.0265	0.4076	0.7483	0.1073	1.8034	0.1601	0.0852	1.3969	0.256
Cordova	0.1937	3.6043	0.0204	**0.3507**	8.1019	0.0002	**0.3826**	9.2951	0.0001
Fairbanks	**0.3115**	6.7867	0.0007	**0.26**	5.271	0.0033	**0.3322**	7.4615	0.0004
Juneau	0.0951	1.5756	0.2084	0.1101	1.856	0.1507	0.1088	1.8311	0.1551
Barter	0.056	0.6927	0.5627	0.0713	0.8963	0.4528	0.0542	0.668	0.5774
Bettles	0.069	1.0631	0.3747	0.0506	0.7635	0.5208	0.1808	3.1625	0.034

Table 5a. Same as Table 4a Except for the Summer Season

Partial r	1950–1998							1950–1988	1952–1998
	Nome	McGrath	Yakutat	Barrow	Cordova	Fairbanks	Juneau	Barter	Bettles
					90–95%				
PNA	−0.1365	0.0821	−0.1401	0.0555	0.0486	0.0166	−0.0681	−0.0336	−0.2258
AO	0.096	−0.1499	−0.0502	−0.0081	−0.0586	−0.1006	0.0142	−0.1592	−0.1792
PDO	0.0218	−0.2404	**−0.3442**	0.0698	−0.1629	**−0.3802**	−0.1921	−0.047	−0.2413
NINO	−0.0556	0.0531	0.1829	−0.1181	0.0753	−0.1293	0.243	−0.0835	−0.0991
					95–100%				
PNA	−0.0362	0.0472	−0.1247	0.0613	−0.1107	0.1607	0.012	0.079	−0.1432
AO	**0.3544**	0.1871	−0.0524	−0.063	0.0537	0.1798	−0.0429	*0.2903*	0.1476
PDO	0.0091	−0.1936	−0.161	−0.0208	0.1417	−0.2216	−0.2312	−0.2451	0.0201
NINO	−0.0026	*0.244*	0.1045	−0.0566	0.0644	0.1555	0.1567	−0.1233	−0.0645
					Mean				
PNA	−0.0699	0.0511	−0.2026	0.0847	−0.1308	0.1556	0.0295	0.0477	**−0.3**
AO	**0.3451**	0.15	−0.0501	0.0135	−0.0359	0.1558	−0.0582	0.2637	0.1585
PDO	−0.0121	−0.1788	*−0.3043*	0.0319	−0.0268	**−0.3459**	*−0.2721*	−0.2567	−0.0653
NINO	0.008	0.2311	0.1578	−0.0688	0.1525	0.1752	0.2032	−0.0646	0.1958

variability of those indices (i.e., the PDO) largely characterized by decadal timescale variability. The multivariate regression of the standardized indices yields normalized partial regression coefficients which measure the relative variance explained independently by each of the four indices. The analyses were performed separately for both winter and summer season (though, as noted earlier, the winter NINO3 series is used for both winter and summer season analyses). The analyses were also performed for both raw and detrended versions of the predictor and predictand time series to evaluate the influence of trends on the results of the analysis. While some serial correlation was present in the detrended time series, this did not significantly modify the estimated significance (α) of the regression coefficients.

[15] Though the regression analysis does not assume statistically independent indicators, it does assume that the indices are linear indicators of the transformed precipitation variations. It is possible that this assumption is not strictly valid. *Gershunov and Barnett* [1998], for example, argue that the PDO modulates ENSO influences on North American precipitation, wherein combination of a warm (cool) PDO and warm (cool) ENSO strengthens ENSO influences, while a destructive match (warm-cold) weakens ENSO influences. If the PDO and ENSO indeed combine to influence precipitation patterns through an interaction between, rather than superposition of, their individual influences, a multivariate linear regression is likely to underestimate the strength of influence of the associated climate forcing on the precipitation patterns of interest.

3.2. Analysis of Large-Scale Circulation

[16] The large-scale seasonal patterns of lower tropospheric (700 hPa) geopotential heights are analyzed for their apparent relationship with the candidate predictors discussed in section 3.1 based on an analysis of the correlation maps of these indices against the 700 hPa field, and analysis of the long-term trend patterns. Finally, the large-scale circulation patterns associated with "extreme" (or "heavy") precipitation events at the various locations in Alaska analyzed are evaluated by compositing the 700 hPa heights for the list of days that exceed the appropriate (e.g., 95th percentile) threshold. An "anomaly" composite is determined through subtraction of the appropriate seasonal 700 hPa seasonal climatology from the actual composite. Comparisons of the spatial patterns from these different analyses (see section 4 below) provide insights into the relationships between trends and variability in mean and extreme precipitation in Alaska, and the potential large-scale influences on these relationships.

4. Results and Discussion

[17] The four modes of climate variability analyzed (AO, PDO, PNA, and ENSO) leave distinctly different impres-

Table 5b. Same as Table 4b Except for the Summer Season

| Statistics	90–95%			95–100%			Cumulative Mean		
	R-Squared	*f* Ratio	*p*	R-Squared	*f* Ratio	*p*	R-Squared	*f* Ratio	*p*
Nome	0.0312	0.4833	0.6956	0.1257	2.1556	0.1065	0.1282	2.2052	0.1005
McGrath	0.0625	0.9996	0.4018	0.1344	2.3282	0.0872	0.1078	1.812	0.1586
Yakutat	0.1253	2.1494	0.1072	0.0383	0.5977	0.6198	0.119	2.0261	0.1237
Barrow	0.0176	0.2683	0.8479	0.011	0.1668	0.9182	0.0111	0.1691	0.9167
Cordova	0.027	0.4161	0.7423	0.04	0.625	0.6026	0.0384	0.5985	0.6193
Fairbanks	0.1691	3.0536	0.0379	0.1437	2.5165	0.0702	**0.2103**	3.9957	0.0132
Juneau	0.0776	1.2618	0.2989	0.0565	0.8975	0.4499	0.0839	1.3743	0.2628
Barter	0.0373	0.4524	0.7172	**0.2176**	3.2439	0.0335	0.1851	2.6507	0.0639
Bettles	0.1224	1.9987	0.1284	0.0462	0.694	0.5608	0.1527	2.5823	0.0657
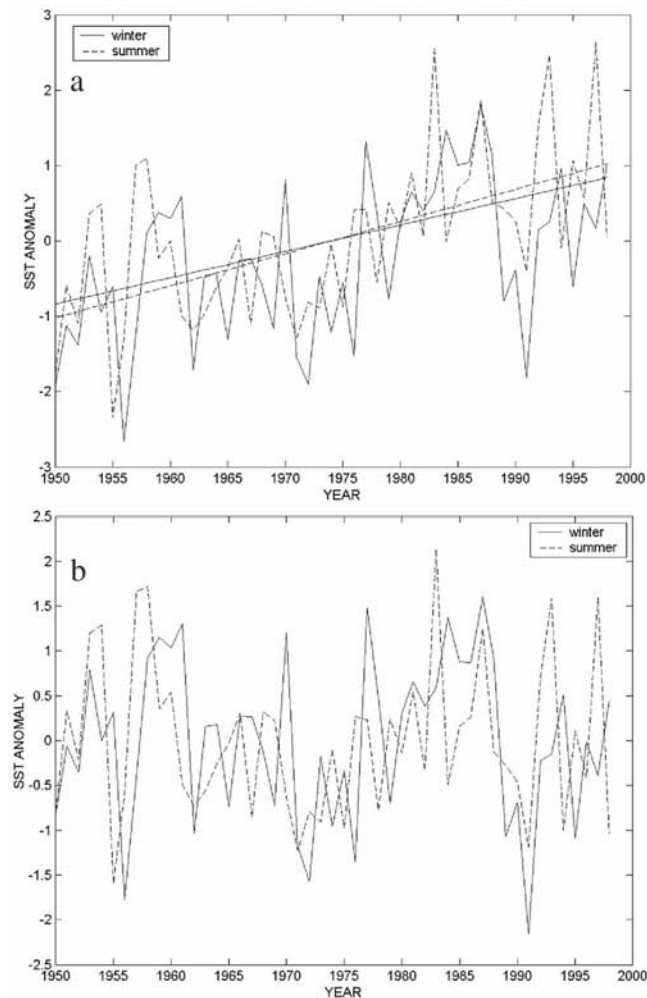
Figure 5. Time series of the seasonal (winter and summer) PDO, both (a) undetrended and (b) detrended (in the former case also showing the linear trend through the series).

sions on the 700 hPa circulation field during the winter and summer seasons (Figures 3–4). The winter season versions of these modes generally imply a stronger impact on the extratropical circulation, consistent with the greater baroclinicity during the winter season (Figure 3). Three of the four winter season indices suggest an anomalous cyclonic circulation that, in the positive (negative) phase, reinforces (weakens) the cyclonic Aleutian Low. Summer season indices leave a more varied signature on the extratropical circulation field, and aside from the AO, the magnitude of the correlations are roughly half that for the winter season (Figure 4).

4.1. Multivariate Analysis of Winter and Summer Precipitation

[18] The four indices (AO, PDO, PNA, and ENSO) have notable trends over the 1950–1998 time period during the summer and winter seasons (Table 1), and the possible leverage exerted by such trends on the results of a multivariate regression must be accounted for. We deal with this issue through a parallel analysis employing the detrended predictors. The results of the multivariate

regression analyses are summarized in Tables 2a–5b. First, the undetrended transformed precipitation is compared against the standardized, undetrended climate indices (Tables 2a–3b). The winter season analyses appear to indicate a highly significant relationship between extreme precipitation with the AO at all stations except the northernmost stations: Barrow, Barter Island, Bettles, and Fairbanks. The same relationship is at least marginally significant (i.e., at least at the 90% level) for mean precipitation. The winter PNA, rather than the winter PDO, appears to exhibits a strong (statistically significant) positive correlation with precipitation at the stations located in south-central regions of Alaska (mean, heavy, extreme), consistent with previous work identifying the PNA, rather than the PDO, as the primary predictor of winter snow accumulation in Mt Logan, which is located in the vicinity of Yakutat [*Moore et al.*, 2002]. The NINO3 index exhibits a statistically significant negative correlation with extreme and mean precipitation at the southern coastal stations. The PDO appears to exhibit little influence on either mean or extreme winter precipitation. For the summer season, the PDO appears to exhibit a negative influence on mean and extreme precipitation at Barter Island and a strongly positive relationship with heavy precipitation just to the southwest at Bettles. The AO seems to show a strong relationship with mean and extreme precipitation at Nome and heavy precipitation at Bettles.

[19] It is tempting to conclude from the preceding analysis the existence of a significant influence of the AO on Alaskan seasonal precipitation patterns, and to a lesser degree, the PNA and ENSO (though the NINO3 index) on winter precipitation and the PDO on summer precipitation. However, as noted previously, several indices exhibit linear trends over the time interval considered (see Table 1). The PDO for example, as shown in Figure 5, exhibits a significant positive trend during both the summer and winter during the 1950–1998 time period. As many of the transformed precipitation series analyzed also exhibit statistically significant trends over this timeframe, apparently significant regression coefficients may result simply from the presence of trends in the various series analyzed, rather than any true relationship on interannual and decadal timescales. We thus performed a parallel analysis using detrended series to establish the relationships that indeed hold at interannual and decadal timescales.

[20] The results from the analysis of the detrended data (see Tables 4a–5b) yield more modest statistical relationships between the AO and precipitation series. The latter analysis indicates a statistically significant ($\alpha > 95\%$) summer season relationship between the AO and extreme precipitation for Nome (with a marginally significance relationship suggested for Barter Island) and a negative relationship between the PDO and heavy and mean precipitation at Yakutat and Fairbanks ($\alpha > 95\%$ in both cases).

[21] During the winter season, a strong relationship emerges between the precipitation series and the PNA and NINO3 indices, almost unaltered from the undetrended relationships discussed above. Simple linear correlations between the precipitation series and the NINO3 and PNA indices may be misleading, because of the co-
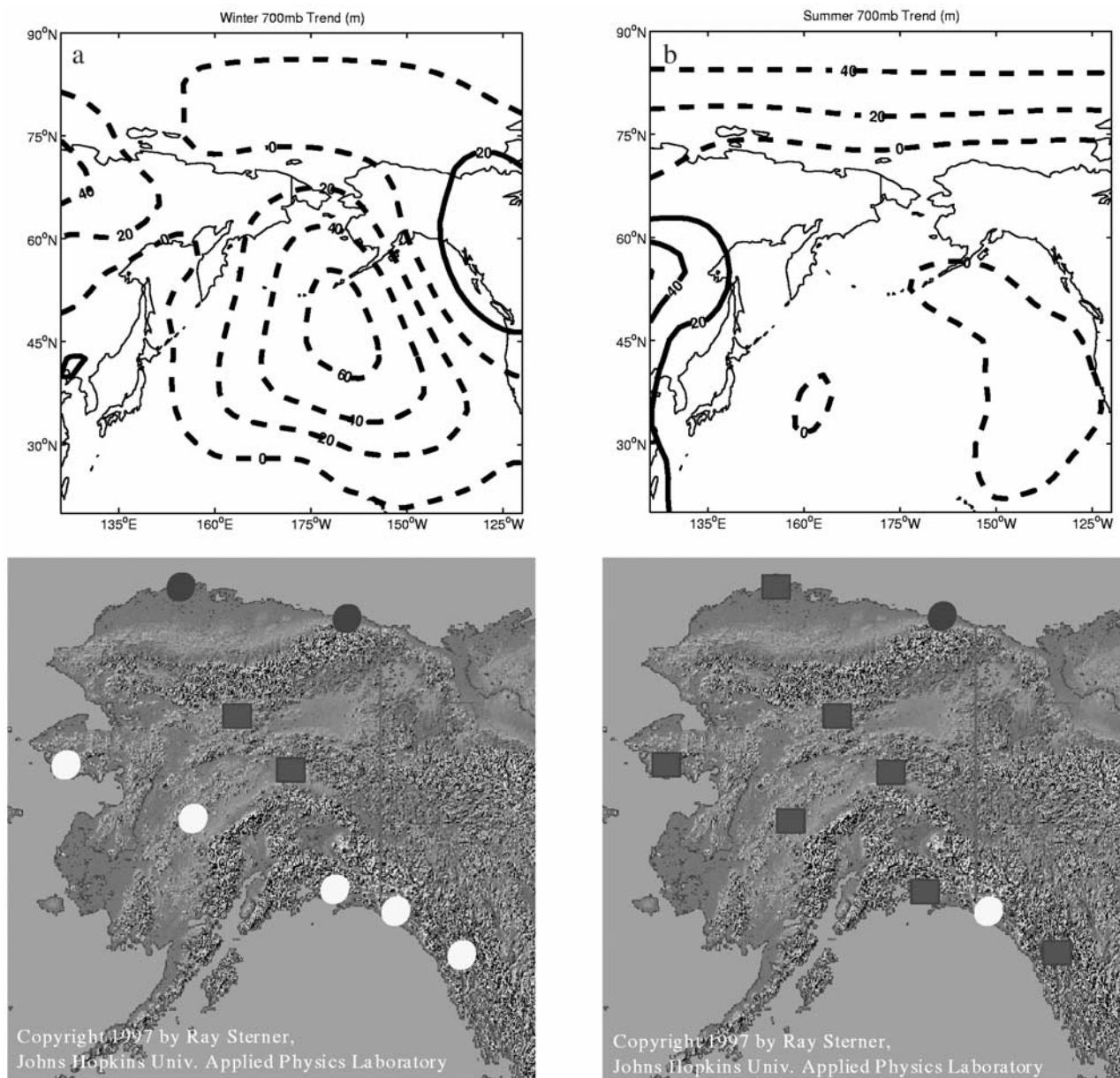
Figure 6. 700 hPa trend pattern during 1950–1998 for the (a) winter season (DJF) and (b) summer season (JJA; negative and zero contours are dashed). The mean precipitation trends are noted for all nine stations superimposed on a high-resolution topographic map of Alaska (topographic map courtesy of Ray Sterner, http://fermi.jhuapl.edu/states/). A white circle indicates a positive trend and a negative trend is noted by a dark circle. All precipitation trends are 95% significant with the exception of McGrath during the winter (greater than 90% significant). Stations with insignificant trends are noted by a square.

linearity present among these two predictors ($r \approx 0.6$) during the winter season. Indeed, the multivariate regression suggests *competing*, rather than like, influences on precipitation. Extreme and mean precipitation appears negatively related to NINO3 at the southeastern coastal stations (Cordova, Yakutat, and Juneau), while a positive relationship between precipitation and the PNA appears to emerge at Cordova and Yakutat ($\alpha > 95\%$). The PNA also appears to influence precipitation negatively at the more inland stations of Fairbanks and McGrath ($\alpha > 95\%$), presumably due a rain shadow effect, as discussed below. A link is evident between trends in mean and heavy

precipitation during the summer season, while mean precipitation is more closely tied to extreme precipitation events during the winter season. The AO and PDO, in summary, appear to be useful determinants of precipitation characteristics during the summer season, while the PNA and NINO3 appear to be determinants during the winter season.

4.2. Large-Scale Circulation Climatology and Precipitation Trends

[22] It is not possible to determine from statistical regression whether a trend in the precipitation data can be
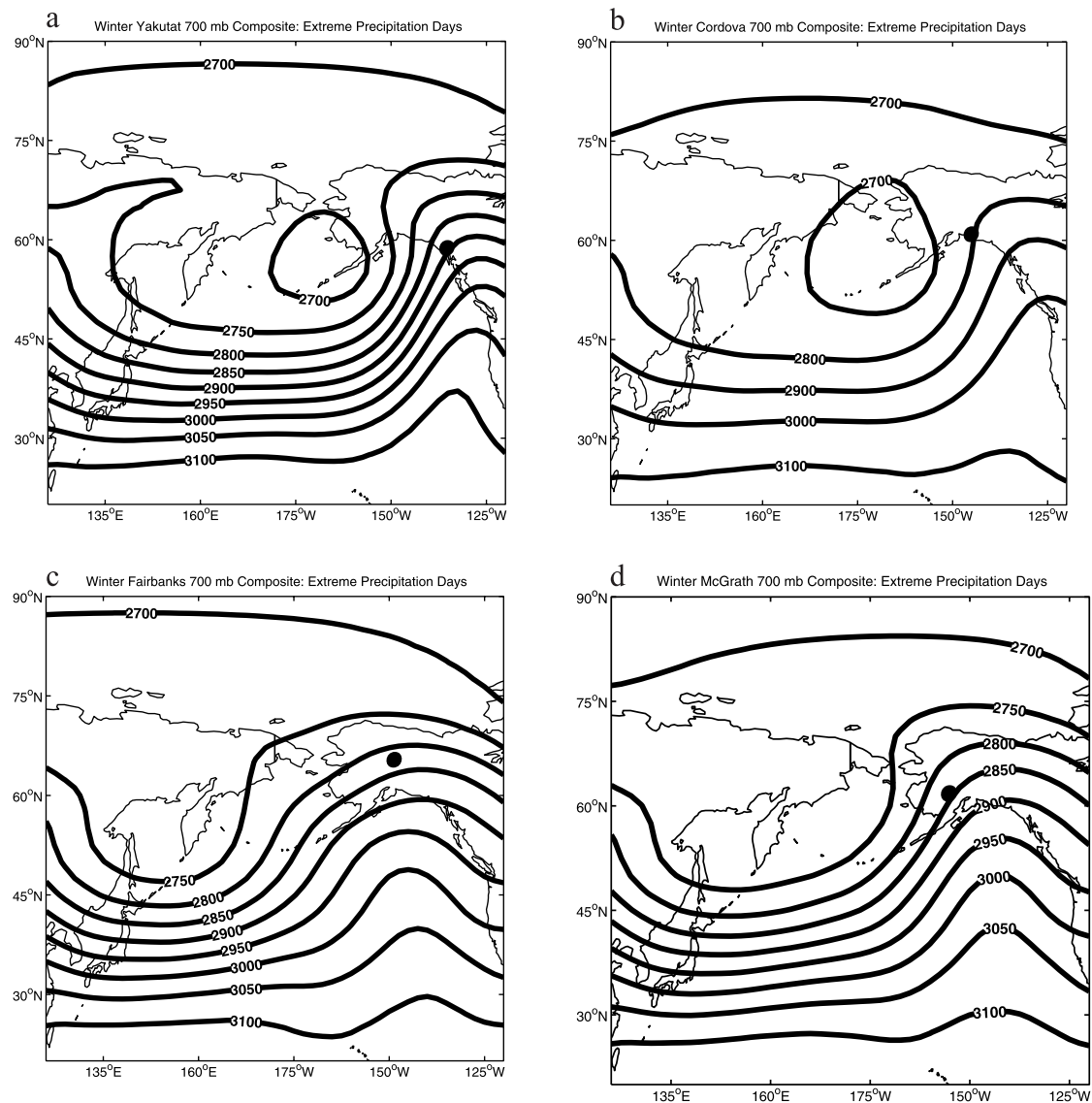
Figure 7. 700 hPa composite patterns during the winter season for extreme precipitation days at (a)Yakutat (b) Cordova (c) Fairbanks (d) McGrath. Station location is noted by a black mark.

attributed to a trend in any particular predictor or set of predictors (e.g., the AO and PDO index). However, an examination of the pattern of trend in the large-scale atmospheric circulation field may nonetheless provide some insight into the possible dynamical factors underlying the observed trends. While we determine trend patterns from the NCEP 700 hPa data, we note that similar patterns of trend (i.e., those consistent with the inferred changes in circulation) are evident in analyses (not shown) of an independent instrumental sea-level pressure (SLP) data set [*Trenberth and Paolino*, 1980]. The latter data are less likely to suffer from the potential limitations of the NCEP data with respect to the estimation of long-term trends discussed earlier.

[23] During the winter, the (700 hPa) circulation clima-tology indicates a broad trough over the west-central sections of the North Pacific, and there is also a distinct ridge over southeastern Alaska and western Canada (Figures 2a–2b). The trend in the 700 hPa pattern

indicates a strengthening trough over the Aleutian Islands and a pronounced strengthening of the western Canadian ridge (Figure 6a). The trend pattern closely resembles the positive PNA geopotential anomaly pattern (see Figure 3a), but also shares certain features (e.g., through a zonal north-south geopotential height contrast component) with the Nino3 geopotential anomaly pattern (see Figure 3b). An anomalous southerly maritime flow into the southern regions of Alaska is indicated, consistent with the potential for greater precipitation and greater extreme precipitation (which benefits in particular from warm maritime air with its greater potential for release of precipitable moisture upon cooling).

[24] The significance of (transformed) precipitation trends is determined based on a two-tailed t-distribution. The winter precipitation data show a broadly significant trend across Alaska, with a clear north-south contrast in the sign of the trend (with no significant trends evident at the centrally located stations of Fairbanks and Bettles)
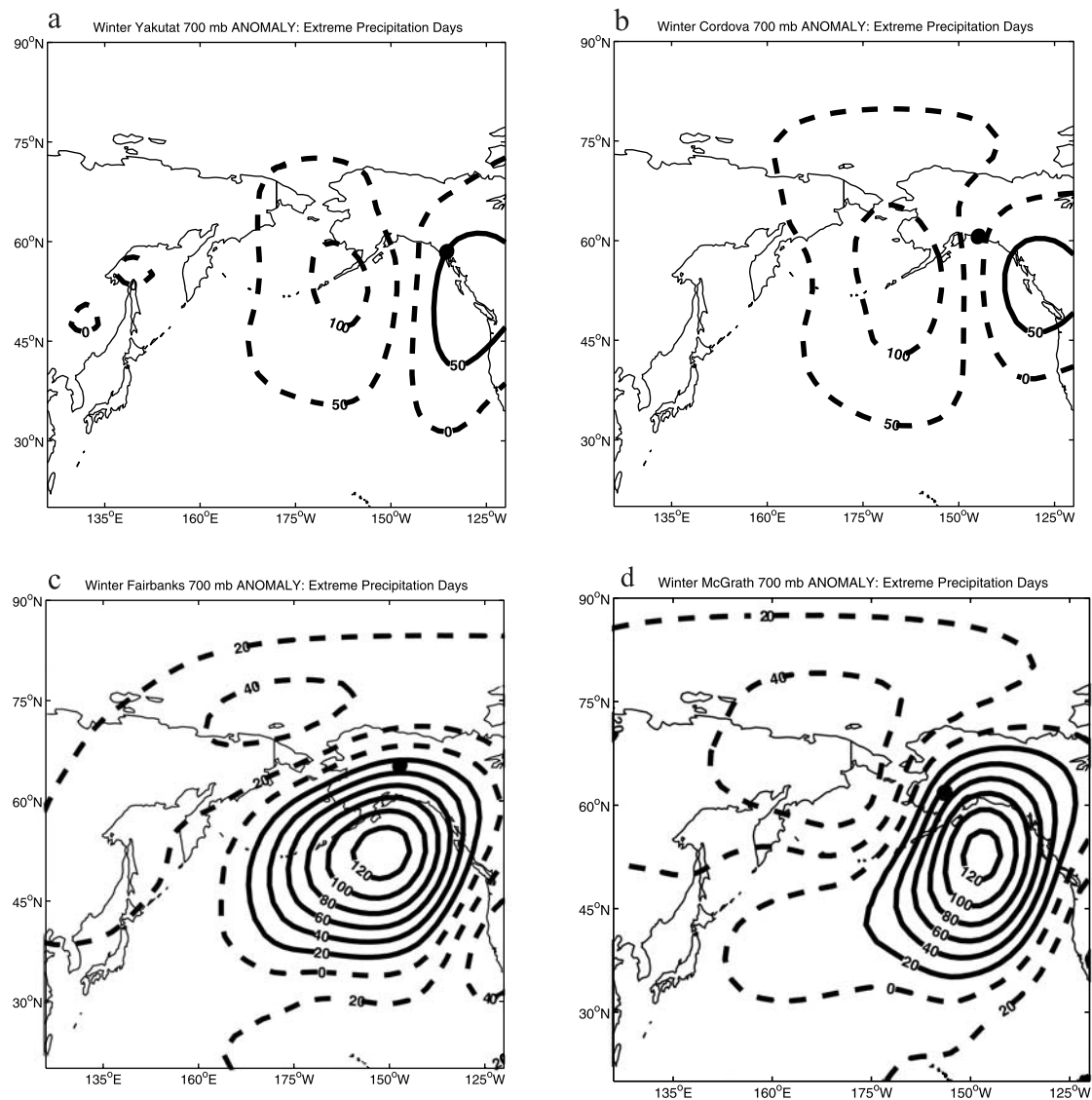
Figure 8. 700 hPa anomaly patterns for winter season extreme precipitation days for the corresponding stations as noted in Figure 7 (negative and zero contours are dashed).

(Figure 6). A significant, positive wintertime trend ($\alpha > 95\%$) is evident along the southern coast (all three stations, Cordova, Yakutat, and Juneau). The western stations of McGrath and Nome also exhibit a positive trend in precipitation ($\alpha > 90\%$ and $\alpha > 95\%$ respectively). Both north slope stations indicate negative winter precipitation trends significant at the 95% level. *Curtis et al.* [1998] suggested that a decrease in the variability of sea-level pressure, and wind direction changes may serve to explain precipitation trends on the north slope. To summarize, the pattern of trend in the winter, transformed precipitation data is consistent with the 700 hPa anomaly pattern, which is suggestive of enhanced advection of warm, maritime air into Alaska along the southern coast, and enhanced southerly flow of dry, cold continental into the north slope region. A nearly identical pattern of trend (not shown) for the extreme precipitation category suggests that the same large-scale atmospheric circulation changes are responsible for simultaneous changes in extreme precipitation trends. The winter

season heavy precipitation category shows similar trends (not shown).

[25] During the summer, the (700 hPa) circulation climatology is characterized by a less discrete trough-ridge pattern over the northern Pacific and central Alaska (Figures 2c–2d). Figure 6b shows that summer 700 hPa trends are weaker, aside from a well-defined decrease in pressure north of 75°N [see also *Walsh et al.*, 1996]. The trend pattern appears analogous to the negative, zonal geopotential heights illustrated by the AO north of 75°N and the cyclonic circulation anomalies in the eastern Pacific as suggested by both the PDO and AO (see Figure 4). The northern zonal anomaly indicates that the northern regions of Alaska may be subjected to increased westerlies.

[26] However, the anomalous circulation trend does not appear to be significant enough to provide an explanatory role in observed Alaskan summer precipitation trends. No significant trends are observed in summer precipitation with
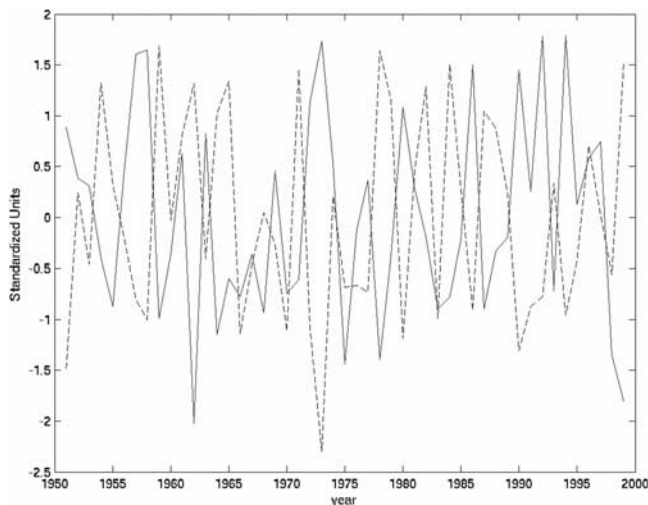
Figure 9. Time series of the winter transformed and detrended extreme precipitation series for McGrath (solid line) compared with the winter detrended PNA index (dashed line).

the exceptions of Yakutat ($\alpha > 95\%$) and Barter Island ($\alpha > 95\%$) (Figure 6b). The trend in extreme precipitation at Yakutat and Barter Island is slightly greater than for mean precipitation (not shown). The only station exhibiting a significant (positive) trend in heavy precipitation is Juneau ($\alpha > 95\%$).

4.3. Analysis of Large-Scale Circulation During Heavy and Extreme Precipitation Days

[27] In order to better understand the relationships between precipitation variations and large-scale atmospheric influences, we examine the large-scale circulation (as inferred from correlation maps of the 700 hPa field) associated with the various seasonal circulation indices. The correlation map for the winter PNA indicates a strong negative relationship south of the Aleutian Islands accompanied by a maximum along western North America (Figure 3a). This pattern is spatially similar to the pattern of (49-year) trend in winter 700 hPa heights (Figure 6a), with the associated negative Aleutian geopotential height anomaly consistent with enhanced southerly flow and stronger advection of coastal moisture near Cordova and Yakutat, and an orographic drying in the lee of the coast range near Fairbanks and McGrath. As discussed earlier, Cordova and Yakutat exhibit positive winter precipitation trends, consistent with significant advection into coastal Alaska.

[28] A composite of extreme winter precipitation days at Yakutat reveals an enhanced trough adjacent to the southwestern coast and a pronounced ridge over far southeast Alaska and the northwest coast (Figure 7a). The anomalous dipole-like pattern is similar to the circulation associated with the positive PNA and to the trend in winter 700 hPa geopotential heights (Figure 6a), suggesting strong southerly onshore advection of moisture toward the coast (Figure 8a). The coastal station of Cordova, located to the west, also indicates a circulation pattern conducive to the onshore advection of moisture (Figures 7b and 8b).

The atmospheric circulation pattern associated with extreme precipitation is thus consistent with a PNA contribution to the positive trend in extreme precipitation.

[29] While the positive PNA pattern seems to be associated with increased extreme precipitation, the NINO3 index, as discussed earlier, appears to exert a distinct, *negative* influence. The correlation map of the winter NINO3 and 700 hPa field highlights an elongated cyclonic circulation reminiscent of the PNA (Figure 3b). However, unlike the PNA, an anomalous enhanced pressure gradient is not inferred along the southeast Alaskan coast. It appears that the El Nino influence neutralizes the ridge associated with winter climatology, the PNA, and the 700 hPA trend, which thereby diminishes extreme and mean precipitation at the coastal stations of Cordova, Yakutat, and to a lesser extent, Juneau.

[30] Converse to the pattern indicative of high winter precipitation in coastal Alaska, composites of extreme winter precipitation days at McGrath and Fairbanks show an anomalous enhanced trough in the western Pacific with a pronounced ridge centered over Alaska (Figures 7c–7d). Figures 8c and 8d illustrate the accompanying anticyclonic 700 hPa anomaly associated with the extreme precipitation days at McGrath and Fairbanks. The anomalous circulation reveals that large winter precipitation events in interior Alaska appear to be associated with south-westerly flow up the Yukon River Valley, favoring the ability of moisture to bypass not only the coastal mountains but also the Alaska Range. The circulation pattern resembles the negative PNA (Figures 3a and 6a). Comparison of the time series of detrended winter precipitation at McGrath and detrended winter PNA illustrates a clear negative relationship (correlation coefficient: −0.60) (Figure 9).

[31] The summer season spatial signatures in circulation, closely associated with the AO and PDO differ markedly from the winter circulation counterparts. The correlation map of the summer AO and 700 hPa heights show a pattern very similar to the summer trend in 700 hPa circulation except that the AO pattern shows a more southerly trough stretching across northern Alaska (Figures 4a and 6b). Similar to the AO pattern, an anomalously deep trough is associated with the composite of extreme precipitation at Nome (Figure 10a). The composite 700 hPa anomaly pattern for extreme precipitation days is suggestive of a dipole structure, which reinforces flow from the southwest and advects moisture toward Nome (Figure 11a). The composite anomaly pattern is thus consistent with the previous results from multivariate regression of candidate indices.

[32] The correlation pattern for the summer PDO indicates a banded circulation structure, with a broad minimum stretching through the central North Pacific (Figure 4b). Increases in heavy precipitation at both Yakutat and Fairbanks are thus consistent with a negative PDO influence, consistent with the previous multivariate regression results. The composite for Yakutat heavy precipitation indicates a deep trough through western Alaska (Figure 10b), while the composite anomaly indicates an anomalous cyclonic minimum centered over south-central Alaska (Figure 11b). The anomalous geopotential gradient implies a greater tendency for moist, southerly flow into the Yakutat region. The same analysis for Fairbanks indicates a less dramatic circulation anomaly (Figure 11c), with the composite map suggesting a
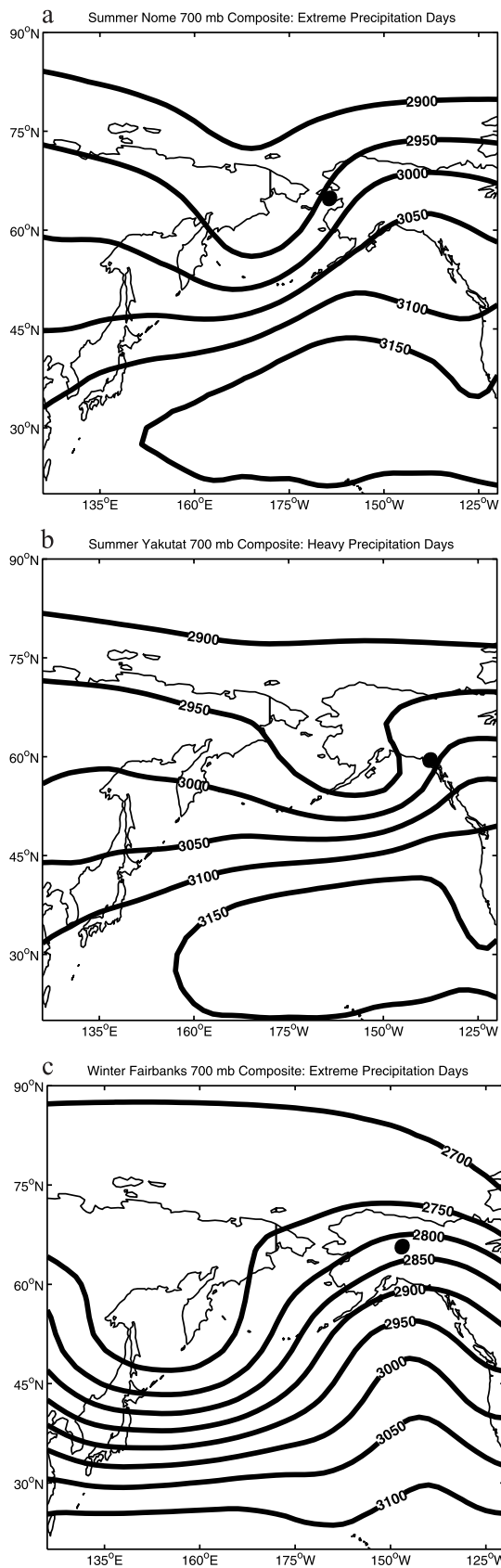
Figure 10. 700 hPa composite patterns during the summer season for extreme precipitation days at (a) Nome and heavy precipitation days at (b) Yakutat (c) Fairbanks. Station location is noted by a black mark.
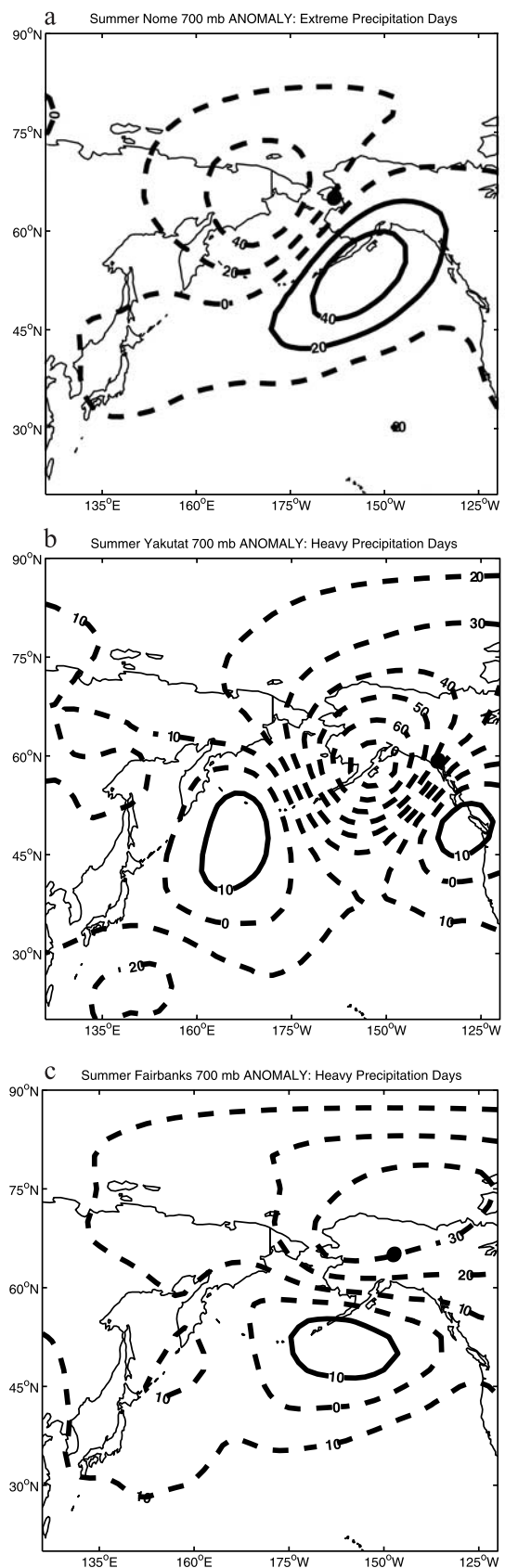
Figure 11. 700 hPa anomaly patterns for summer season precipitation days for the corresponding stations as noted in Figure 10 (negative and zero contours are dashed).

more banded trough within Alaska, which could be reflective of a negative PDO-like pattern (Figure 10c). Differences between Fairbanks and Yakutat are nonetheless difficult to reconcile with any simple interpretation involving a PDO influence.

5. Conclusions

[33] During the winter, coastal and interior Alaskan precipitation variability appears to be closely coupled with the variations of the PNA, while ENSO appears to predominately influence coastal Alaska. The winter trends in the mean, heavy, and extreme precipitation during the latter 20th century within interior and coastal Alaska confirm the expectation that anomalous southerly-to-southwesterly flow over southern Alaska favors increased precipitation totals and precipitation intensity, through increased advection of warm moist air into coastal regions. Coastal orography clearly plays an important role, with strong onshore coastal flow leading to decreased precipitation at interior stations (e.g., Fairbanks and McGrath). Coastal precipitation trends are consistent with previously identified [*Cayan and Peterson*, 1989] anomalous streamflow trends along the southern coast of Alaska. Increased southerly advection has also been linked to anomalously warm surface air temperatures over the 1954–2000 time period [*Papineau*, 2001].

[34] Noteworthy in our analysis is the distinction between winter ENSO and PNA influences along southeastern coastal Alaska (Cordova, Yakutat, and Juneau). *Yarnal and Diaz* [1986] found a positive relationship between southeastern Alaska precipitation and ENSO, and argued for the importance of the PNA pattern in advecting moisture toward the coast. Our multivariate regression analysis suggests, instead, an opposing influence of the PNA and ENSO on coastal precipitation. Although the extratropical ENSO influence and the PNA have similar spatial characteristics, the absence of a ridge in western Canada associated with the NINO3 pattern may decrease the strong steering currents associated with the PNA and 700 hPa trend.

[35] The 49-year 700 hPa trend bears a striking spatial resemblance to a combination of the wintertime, cyclonic PNA and the more elongated NINO3 pattern, suggesting that recent winter circulation changes along coastal Alaska are being modulated by a combination of the two indices. Our analysis does not reveal any significant winter PDO influence on precipitation on interannual-through decadal timescales, contrasting with previous findings emphasizing multidecadal timescales relationships in the Gulf of Alaska region [*Mantua et al.*, 1997].

[36] For the north slope region, negative precipitation trends are more difficult to reconcile with any direct influences by the PNA or ENSO. Anomalous southerly flow may increasingly be leading to drying of the region via a rain shadow affect. Contrary to this interpretation, however, *Stone et al.* [2002] show that moisture transport from the North Pacific is responsible for above normal snowfall north of the Brooks Range. Furthermore, they indicate that maritime flow has become less frequent contributing to less snowfall during the period 1986–2000, suggesting the potential explanatory role of anomalous atmospheric circulation. Our analysis is unable to provide a simple explanation for such anomalous circulation in terms of the key indicators of climate change in the North Pacific region.

[37] Summer season changes are even more challenging to interpret. Summer precipitation trends are of marginal statistical significance with a few exceptions (Yakutat, Barter Island, and Juneau, depending on precipitation category). The trend in summer circulation suggests a zonally symmetric anomalous low-pressure region north of 75°N, reminiscent of the anomalous circulation associated with the positive AO. Composites of geopotential heights associated with heavy precipitation days at Yakutat and Fairbanks suggest a circulation anomaly partially reminiscent of the PDO, but there are also substantial discrepancies with the PDO pattern. The north slope region, again, appears too remote for any consistent AO or the PDO influences.

References

Barnston, A. G., and R. E. Livezey (1987), Classification, seasonality and persistence of low-frequency atmospheric circulation patterns, *Mon. Weather Rev.*, *115*, 1083–1126.

Bowling, S. A. (1980), The weather and climate of Alaska, *Weatherwise*, *33*, 196–201.

Cayan, D. R., and D. H. Peterson (1989), The Influence of North Pacific atmospheric circulation on streamflow in the west, *Geophys. Monogr.*, *55*, 368–375.

Curtis, J., G. Wendler, R. Stone, and E. Dutton (1998), Precipitation decrease in the western Arctic with special emphasis on Barrow and Barter Island, Alaska, *Int. J. Climatol.*, *18*, 1687–1707.

Daly, C., R. P. Neilson, and D. L. Phillips (1994), A statistical-topographic model for mapping climatological precipitation over mountainous terrain, *J. Appl. Meteorol.*, *33*, 140–158.

Doherty, R. M., M. Hulme, and C. G. Jones (1999), A gridded reconstruction of land and ocean precipitation for the extended tropics from 1974–1994, *Int. J. Climatol.*, *19*, 119–142.

Folland, C. K., T. R. Karl, J. R. Christy, R. A. Clarke, G. V. Gruza, J. Jouzel, M. E. Mann, J. Oerlemans, M. J. Salinger, and S. W. Wang (2001), Observed climate variability and change, in *Climate Change 2001: The Scientific Basis*, edited by J. T. Houghton et al., pp. 99–181, Cambridge Univ. Press, New York.

Gershunov, A., and T. Barnett (1998), Interdecadal modulation of ENSO teleconnections, *Bull. Am. Meteorol. Soc.*, *79*, 2715–2726.

Groisman, P. Y., and D. R. Easterling (1994), Variability and trends of total precipitation and snowfall over the United States and Canada, *J. Clim.*, *7*, 184–205.

Hulme, M., T. J. Osborn, and T. C. Johns (1998), Precipitation sensitivity to global warming: comparison of observations with HadCM2 simulations, *Geophys. Res. Lett.*, *25*, 3379–3382.

Hurrell, J. W., and K. E. Trenberth (1998), Difficulties in obtaining reliable temperature trends: Reconciling the surface and satellite microwave sounding unit records, *J. Clim.*, *11*, 945–967.

Hurrell, J. W., and H. van Loon (1997), Decadal variations in climate associated with the North Atlantic Oscillation, *Clim. Change*, *36*, 301–326.

Jones, P. D., M. New, D. Parker, S. Martin, and J. Rigor (1999), Surface air temperature and its changes over the past 150 years, *Rev. Geophys.*, *37*, 173–199.

Kalnay, E. (1996), The NCEP/NCAR 40-year reanalysis project, *Bull. Am. Meteorol. Soc.*, *77*, 437–471.

Karl, T. R., and R. W. Knight (1998), Secular trends of precipitation amount, frequency, and intensity in the United States, *Bull. Am. Meteorol. Soc.*, *79*, 231–241.

Katz, R. W., and B. G. Brown (1992), Extreme events in a changing climate: Variability is more important than averages, *Clim. Change*, *21*, 289–302.

Kistler, R., et al. (2001), The NCEP-NCAR 50-year reanalysis: Monthly means CD-ROM and documentation, *Bull. Am. Meteorol. Soc.*, *82*, 247–268.

Livezey, R. E., and K. C. Mo (1987), Tropical-extratropical teleconnections during the Northern Hemisphere winter. part II: Relationships between monthly mean Northern Hemisphere circulation patterns and proxies for tropical convection, *Mon. Weather Rev.*, *115*, 3115–3132.

Mantua, N. J., and S. R. Hare (2002), The Pacific decadal oscillation, *J. Oceanogr.*, *58*, 35–44.

Mantua, N., S. Hare, Y. Zhang, J. Wallace, and R. Francis (1997), A Pacific interdecadal oscillation with impacts on salmon production, *Bull. Am. Meteorol. Soc.*, *76*, 1069–1079.

Miller, A. J., and N. Schneider (2000), Interdecadal climate regime dynamics in the North Pacific Ocean: Theories, observations and ecosystem impacts, *Prog. Oceanogr.*, *47*, 355–379.

Moore, G. W. K., G. Holdsworth, and K. Alverson (2002), Climate change in the North Pacific region over the past three centuries, *Nature*, *420*, 401–403.

Papineau, J. M. (2001), Wintertime temperature anomalies in Alaska correlated with ENSO and PDO, *Int. J. Climatol.*, *21*, 1577–1592.

Paulson, R. W., E. B. Chase, R. S. Roberts, and D. W. Moody (1991), 1988–89-Hydrologic events and floods and droughts, *U.S. Geol. Surv. Water Supply Pap. 2375*, Reston, Va.

Renshaw, A. C., D. P. Rowell, and C. K. Folland (1998), Wintertime low-frequency weather variability in the North Pacific—American sector 1949–93, *J. Clim.*, *11*, 1073–1093.

Stone, R. S., E. G. Dutton, J. M. Harris, and D. Longenecker (2002), Earlier spring snowmelt in northern Alaska as an indicator of climate change, *J. Geophys. Res.*, *107*(D10), 4089, doi:10.1029/2000JD000286.

Thompson, D. W. J., and J. M. Wallace (1998), The Artic Oscillation signature in the wintertime geopotential height and temperature fields, *Geophys. Res. Lett.*, *25*, 1297–1300.

Thompson, D. W. J., and J. M. Wallace (2000), Annular modes in the extratropical circulation. part I: Month-to-month variability, *J. Clim.*, *13*, 1000–1016.

Trenberth, K. E. (1990), Recent observed interdecadal climate changes in the Northern Hemisphere, *Bull. Am. Meteorol. Soc.*, *71*, 988–993.

Trenberth, K. E. (1997), The Definition of El Niño, *Bull. Am. Meteorol. Soc.*, *78*, 2771–2777.

Trenberth, K. E., and J. W. Hurrell (1994), Decadal atmosphere-ocean variations in the Pacific, *Clim. Dyn.*, *9*, 303–319.

Trenberth, K. E., and D. A. Paolino (1980), The Northern Hemisphere sea-level pressure data set: Trends, errors and discontinuties, *Mon. Weather Rev.*, *108*, 855–872.

Wallace, J. M., and D. S. Gutzler (1981), Teleconnections in the geopotential height field during the Northern Hemisphere winter, *Mon. Weather Rev.*, *109*, 784–812.

Walsh, J. E., W. L. Chapman, and T. L. Shy (1996), Recent decrease of sea level pressure in the central Arctic, *J. Clim.*, *9*, 480–486.

Watson, R. T. (Ed.) (2001), *Climate Change 2001: Synthesis Report*, Cambridge Univ. Press, New York.

Yarnal, B., and H. F. Diaz (1986), Relationships between extremes of the Southern Oscillation and the winter climate of the Anglo-American Pacific coast, *J. Climatol.*, *6*, 197–219.

————————

B. I. Cook and M. E. Mann, Department of Environmental Sciences, University of Virginia, Charlottesville, VA 22903, USA. (bc9z@virginia.edu; mann@virginia.edu)

B. E. Gleason and R. S. Vose, National Climatic Data Center, NOAA/National Environmental Satellite Data and Information Service, 151 Patton Ave., Asheville, NC 28801, USA. (byron.gleason@noaa.gov; russell.vose@noaa.gov)

M. L. L'Heureux, Department of Atmospheric Science, Colorado State University, Fort Collins, CO 80523, USA. (michl@atmos.colostate.edu)